Biochemical Journal (2017) **474** 2219–2233
DOI: 10.1042/BCJ20170173

PORTLAND PRESS

Research Article

Comparative functional analysis of ribonuclease 1 homologs: molecular insights into evolving vertebrate physiology

Jo E. Lomax[1,*], Chelcie H. Eller[2,*] and Ronald T. Raines[2,3]

[1]Graduate Program in Cell and Molecular Biology, University of Wisconsin-Madison, 1525 Linden Drive, Madison, WI, U.S.A.; [2]Department of Biochemistry, University of Wisconsin-Madison, 433 Babcock Drive, Madison, WI, U.S.A.; and [3]Department of Chemistry, University of Wisconsin-Madison, 1101 University Avenue, Madison, WI, U.S.A.

Correspondence: Ronald T. Raines (rtraines@wisc.edu)

Pancreatic-type ribonucleases (ptRNases) comprise a class of highly conserved secretory endoribonucleases in vertebrates. The prototype of this enzyme family is ribonuclease 1 (RNase 1). Understanding the physiological roles of RNase 1 is becoming increasingly important, as engineered forms of the enzyme progress through clinical trials as chemotherapeutic agents for cancer. Here, we present an in-depth biochemical characterization of RNase 1 homologs from a broad range of mammals (human, bat, squirrel, horse, cat, mouse, and cow) and nonmammalian species (chicken, lizard, and frog). We discover that the human homolog of RNase 1 has a pH optimum for catalysis, ability to degrade double-stranded RNA, and affinity for cell-surface glycans that are distinctly higher than those of its homologs. These attributes have relevance for human health. Moreover, the functional diversification of the 10 RNase 1 homologs illuminates the regulation of extracellular RNA and other aspects of vertebrate evolution.

Introduction

Vertebrate animals possess a distinct, conserved family of secreted ribonucleases (RNases) not known to occur in any other taxon. This unique group of enzymes is termed the pancreatic-type RNases (ptRNases) or, alternatively, the vertebrate secretory RNases. They are not homologous to any other class of eukaryotic RNases and together constitute an extensive superfamily of proteins that has been the subject of intense biochemical, structural, and evolutionary studies for over half a century. With compact structures, high stability, and a shared ability to catalyze the nonspecific degradation of RNA, these small and hardy enzymes are purported to serve a variety of diverse biological roles *in vivo*, including supporting host defense and innate immunity [1,2]. Indeed, numerous phylogenetic reconstructions and other analyses indicate that the family is evolving and expanding rapidly, and that many members are under positive selection for increased functional diversification, as is common with immunity-related protein families [3–6]. The various activities of ptRNases are regulated by the cytosolic RNase inhibitor (RI) protein, which is conserved across various species and can bind extremely tightly to ptRNases, inhibiting their catalytic activity [7,8].

The most well-known member of the ptRNase family is RNase 1. (Cow RNase 1 is also known as RNase A and has served as a model protein for countless advances in biological chemistry [9–11].) Of all the ptRNases, RNase 1 has the highest catalytic activity, as well as the most diverse and robust expression [1,12]. In addition to its broad tissue expression, RNase 1 has been isolated from a large variety of bodily fluids [12,13]. In humans and mice, RNase 1 circulates freely in the blood and serum at a concentration of ~0.5 μg/ml and is the only known RNase in plasma with high, nonspecific ribonucleolytic activity [14–17]. Secreted RNase 1 also possesses the ability to enter the cytosol of other

*These authors contributed equally to this work.

Received: 3 March 2017
Revised: 30 April 2017
Accepted: 10 May 2017

Accepted Manuscript online: 11 May 2017
Version of Record published: 21 June 2017

Biochemical Journal (2017) **474** 2219–2233
DOI: 10.1042/BCJ20170173

cells via endocytosis and translocation. This remarkable ability has been exploited to create variants of RNase 1 that can act as chemotherapeutic agents against cancer cells [8,18–20], including prototypes now in clinical trials [21,22].

Despite its widespread conservation in mammals and unique properties, the biological role of RNase 1 is poorly understood. Owing to the high level of expression of RNase A in the cow pancreas, RNase 1 was historically known as a digestive enzyme and was thought to serve little purpose in nonruminant mammals, including humans [23]. That impression began to change as studies compiled diverse data suggesting a nondigestive role for RNase 1 in species apart from cattle [24–26]. Correspondingly, phylogenetic analyses have predicted that RNase A diverged relatively recently through gene duplication in ruminants, and might represent a specialized digestive form of the RNase 1 enzyme that arose simultaneously with foregut fermentation [27,28]. Intriguingly, cattle express two other RNase 1 paralogs, which have been shown to have properties distinct from that of RNase A [29,30]. A similar phenomenon is known to have occurred in leaf-eating monkeys, where a secondary form of RNase 1 evolved to participate in ruminant-like digestion [31]. Analogously, modern whales and dolphins, which share a common ancestor with cattle, seemingly lost their extra copies of RNase 1 concurrent to switching from a herbivorous to a carnivorous diet [32]. Taken together, extant evidence suggests that cow RNase A—the original so-called pancreatic RNase—might be a functional outlier among RNase 1 homologs, with the true physiological role of RNase 1 in other vertebrates still to be unveiled.

Previous functional studies of RNase 1 enzyme homologs have uncovered biochemical differences across a limited subset of species [27,30,31,33]. Broader functional differences across species have been predicted through phylogenetic analyses of *RNase1* genes. For example, *RNase1* gene duplication events and differential selection pressures have been uncovered in rodent, carnivore, and bat families, suggesting that new functional roles may be emerging [34–37]. Nonetheless, knowledge of the actual behavior of the RNase 1 enzyme from diverse species represents a critical gap in our understanding of RNase 1 biology.

Comparative functional analyses can illuminate conserved or derived protein functions [38–41]. Such analyses, which bridge the divide between structural biology, biochemistry, and molecular evolution, are critical for advancing our understanding of RNase 1. Here, we present the broadest and most in-depth study, to date, of the function of RNase 1 proteins across a vertebrate evolutionary spectrum, including seven mammalian homologs and three nonmammalian homologs. We build upon an existing framework of phylogenetic analyses by probing the functional diversification of these homologs, as well as speculate on key amino acid changes that might have led to pronounced differences in both biochemical properties and biological function.

Materials and methods

Materials and instrumentation

Escherichia coli BL21(DE3) cells and plasmid pET22b(+) were from EMD Millipore. 6-FAM–dArUdAdA–6-TAMRA, 5,6-FAM–d(CGATC)(rU)d(ACTGCAACGGCAGTAGATCG), and DNA oligonucleotides for PCR, sequencing, and mutagenesis were from Integrated DNA Technologies. Poly(A:U) was from Sigma Chemical; low molecular mass poly(I:C) was from InvivoGen. Sulfatides, phosphatidylserine, and cetyltrimethylammonium bromide (CTAB) were from Avanti Polar Lipids.

Protein purification columns were from GE Healthcare. Restriction and PCR enzymes were from Promega. Ninety-six-well plates were from Corning. 2-(*N*-morpholino)ethanesulfonic acid (MES) was purified to be free of oligo(vinylsulfonic acid) [42]. All other chemicals were of commercial grade or better, and were used without further purification.

The molecular mass of each RNase was determined by matrix-assisted laser desorption/ionization-time-of-flight (MALDI-TOF) mass spectrometry with a Voyager-DE-PRO Biospectrometry Workstation from Applied Biosystems at the campus Biophysics Instrumentation Facility. All fluorescence and absorbance measurements were made with a M1000 fluorimeter plate reader from Tecan, unless stated otherwise. All data were fitted and analyzed using the Prism 5 software from GraphPad, unless stated otherwise.

RNase cloning and purification

Genes encoding human RNase 1 [43], cow RNase 1 [43], mouse RNase 1 [8], chicken RNase A-1 [8], anole RNase [8], and frog RNase [44] had been inserted previously into the pET22b expression vector for tagless expression in BL21(DE3) *E. coli*. A gene encoding bat RNase 1 (GenBank Accession No. AEF13449) was amplified from little brown bat (*Myotis lucifugus*) skin cDNA and inserted into pET22b. Genes encoding cat RNase

1 (GenBank Accession No. XP_003987441) and horse RNase 1 (GenBank Accession No. NP_001296341) were, respectively, amplified from cat and horse liver cDNA libraries (Zyagen Life Sciences) and inserted into pET22b. A gene encoding squirrel RNase 1 (GenBank Accession No. ACV70066) was amplified from *Scurius carolinensis* liver cDNA and inserted into pET22b. The program Signal P was used to predict and exclude peptide leader sequences for all proteins. The nucleotide sequence for each primer used for cloning is listed in Supplementary Table S1.

To enable site-specific fluorophore-labeling of the RNase 1 homologs, cysteine residues were introduced via site-directed mutagenesis into loop regions distal to the enzymic active site. The ensuing variants were P19C human RNase 1, S19C mouse RNase 1, A19C cow RNase 1, S19C horse RNase 1, T18C cat RNase 1, P18C bat RNase 1, S19C squirrel RNase 1, T17C chicken RNase A-1, S20C anole RNase 1, and S61C frog RNase. Recombinant wild-type ptRNases and their variants were purified as inclusion bodies from *E. coli*, and free-cysteine protein variants were labeled with BODIPY FL (Molecular Probes) as described previously [45,46]. Following purification, protein solutions were dialyzed against PBS and filtered prior to use. The molecular masses of RNase conjugates were confirmed by MALDI-TOF mass spectrometry. Protein concentration was determined by using a bicinchoninic acid assay kit (Pierce) with wild-type RNase A as a standard.

Thermostability measurements

The thermal denaturation of RNase 1 homologs was monitored in the presence of a fluorescent dye using differential scanning fluorimetry (DSF). DSF was performed using a ViiA 7 Real-Time PCR machine (Applied Biosystems) as described previously [47,48]. Briefly, a solution of protein (30 μg) was placed in the wells of a MicroAmp optical 96-well plate, and SYPRO Orange dye (Sigma Chemical) was added to a final dye dilution of 1 : 166 in relation to the stock solution of the manufacturer. The temperature was increased from 20°C to 96°C at 1°C/min in steps of 1°C. Fluorescence intensity was measured at 578 nm, and a solution with no protein was used for background correction. Values of T_m were calculated by fitting the ∂fluorescence/∂T data to a two-state Boltzmann model with the Protein Thermal Shift software (Applied Biosystems).

pH dependence of enzyme activity against ssRNA

The pH dependence of k_{cat}/K_M for the cleavage of ssRNA by RNase 1 homologs was determined with a fluorogenic substrate in which a single ribonucleotide residue was embedded in a DNA oligonucleotide with a fluorophore at its 5′-terminus and a quencher at its 3′-terminus: 6-FAM–dArUdAdA–6-TAMRA [49]. Assays were performed at 25°C in solutions of an RNase 1 and 6-FAM–dArUdAdA–6-TAMRA (0.2 μM) in an RNase-free buffer: 0.10 M NaOAc, 0.10 M NaCl (pH 4.0–5.5); 0.10 M Bis–Tris, 0.10 M NaCl (pH 6.0–6.5); 0.10 M Tris, 0.10 M NaCl (pH 7.0–9.0). All assays were performed in triplicate with three different enzyme preparations. Values of optimal pH were calculated by fitting of normalized initial velocity data from solutions of various pH to a bell-shaped distribution. Values of k_{cat}/K_M at the optimal pH were determined from initial velocity data, as described previously [49].

Degradation of double-stranded RNA

The value of k_{cat}/K_M for the cleavage of a double-stranded (ds)RNA by RNase 1 homologs was determined with polymeric substrates by UV spectroscopy, as described previously [33]. Briefly, poly(A:U) (Sigma Chemical) and low molecular mass poly(I:C) (InvivoGen) were dissolved in H_2O to a concentration of 20 mg/ml. Prior to use, 25 μl of a poly(A:U) or poly(I:C) solution was added to 0.50 ml of 0.10 M MES–HCl buffer (pH 7.4) containing NaCl (0.10 M). The resulting solution was added to the wells of a 96-well plate in 2-fold serial dilutions. After equilibration at 25°C, a baseline at A_{260} was established, and the initial substrate concentration was determined by using $\varepsilon_{260\ nm} = 6.5\ mM^{-1}\ cm^{-1}$ for poly(A:U) and $\varepsilon_{260\ nm} = 4.4\ mM^{-1}\ cm^{-1}$ for poly(I:C). RNases were added to the wells, and the change in absorbance at 260 nm was monitored over time. Initial reaction velocities were determined by using $\Delta\varepsilon_{260\ nm} = 3.4\ mM^{-1}\ cm^{-1}$ for poly(A:U) and $\Delta\varepsilon_{260\ nm} = 1.8\ mM^{-1}\ cm^{-1}$ for poly(I:C). All assays were performed in triplicate with three different enzyme preparations. Values of k_{cat}/K_M were calculated by fitting data to the Michaelis–Menten equation.

The degradation of dsRNA was also assessed with a well-defined substrate, as described previously [30]. As in the ssRNA substrate, a single ribonucleotide residue was embedded in a DNA oligonucleotide with a fluorophore at its 5′-terminus: 5,6-FAM–d(CGATC)(rU)d(ACTGCAACGGCAGTAGATCG). Briefly, the substrate was dissolved in water and allowed to form a hairpin by heating to 95°C and then cooling slowly to room temperature. Assay solutions contained an RNase (1.0 μM) and substrate (50 nM) in 0.10 M MES–HCl buffer

Biochemical Journal (2017) 474 2219–2233
DOI: 10.1042/BCJ20170173

(pH 7.4) containing NaCl (0.10 M). Reactions were allowed to proceed for 5 min at 25°C. Reactions were quenched by the addition of 40 units of rRNasin (Promega), and products were subjected to electrophoresis at 10 mA on a native polyacrylamide (20% w/v) gel. The formation of the cleavage product was measured by excitation of FAM at 495 nm and emission at 515 nm with a Typhoon FLA 9000 scanner (GE Healthcare). Band density was quantified from FAM fluorescence with the ImageQuant software (GE Healthcare). The gel was then incubated in SYBR Gold stain (Invitrogen) and imaged for total nucleic acid. All assays were performed in triplicate with three different enzyme preparations.

Native gel-shift analysis of RI·RNase complexes

Human RI and various RNases from endogenous species were incubated in a 1 : 1.2 molar ratio in PBS at 25°C for 20 min to allow for complex formation. A 10-µl aliquot of protein solution was combined with 2 µl of a 6× loading dye, and the resulting mixtures were loaded immediately onto a non-denaturing 12% (w/v) polyacrylamide gel (Bio-Rad). Gels were run in the absence of SDS at 20–25 mA for ∼3 h at 4°C and stained with the Coomassie Brilliant Blue G-250 dye (Sigma Chemical).

Cellular internalization of RNases

The uptake of RNase 1 homologs by mammalian cells was monitored by flow cytometry, as described previously [45]. Human K-562 cells were grown in RPMI medium (Invitrogen) containing fetal bovine serum (10% v/v) and pen/strep (Invitrogen). Cells were maintained at 37°C under 5% (v/v) CO_2 (g). Cells were plated at 2×10^6 cells/ml in a 96-well plate. RNase 1–BODIPY conjugates in PBS were added to a concentration of 5 µM, and the resulting solutions were incubated for 4 h. Cells were collected by centrifugation at 1000 rpm for 5 min, washed twice with PBS, exchanged into fresh medium, and collected on ice. The total fluorescence of live cells was measured with a FacsCalibur flow cytometer (BD Biosciences). Fluorescence data between experiments were normalized by calibrating each run with fluorescent beads and subtracting the background fluorescence upon treatment with PBS lacking an RNase 1 homolog. Data were analyzed with FlowJo software (Tree Star).

Binding of RNases to cell-surface glycans

The affinity of RNase 1 homologs for mammalian cell-surface glycans was assessed with fluorescence polarization, as described previously [30]. Briefly, solutions of heparin, chondroitin sulfate A, and chondroitin sulfate C in PBS (pH 7.4) were added to the wells of a 96-well plate in 5-fold serial dilutions. RNase 1–BODIPY conjugates were added to a concentration of 50 nM, and the resulting solutions were incubated for 30 min at room temperature to achieve equilibrium. Fluorescence polarization was monitored by excitation at 470 nm and emission at 535 nm, and data were normalized to a solution lacking glycan and fitted by nonlinear regression to the following equation:

$$B = \frac{B_{\max}[\text{ptRNase}]^h}{K_d^h + [\text{ptRNase}]^h} \quad (1)$$

where B is the normalized fluorescence, $B_{\max}$ is the maximum fluorescence, and h is a Hill coefficient.

^{1}H,^{15}N-HSQC NMR spectroscopy with RNase 1

[^{15}N]-RNase 1 was produced in *E. coli* as described previously, using a double-growth procedure in minimal medium containing [^{15}N]-NH_4Cl after induction with IPTG [50]. Growth conditions yielded an average of 15 mg of RNase 1 from 1 l of medium. Protein purification was monitored by using SDS–PAGE, and purified protein was analyzed by mass spectrometry using an Applied Biosystems/MDS SCIEX 4800 MALDI-TOF/TOF instrument. The observed mass of 14790.1 Da indicated that isotope incorporation had been 100% × (14 790–14 604)/192 = 97%.

^{1}H,^{15}N-HSQC NMR spectroscopy [51] was performed on 600 µl of 100 mM KH_2PO_4 buffer (pH 6.5 or 4.7) containing [^{15}N]-RNase 1 (250 µM), D_2O (10% v/v), and a molar equivalent of sulfatides, which mimic heparan sulfate (HS; pH 6.5), or phosphatidylserine (PS; pH 4.7) within CTAB micelles (25 mM). NMR spectra were acquired at 25°C with a Bruker Avance III 600 MHz spectrometer. ^{1}H,^{15}N-HSQC NMR data were quantified and peak assignments were made with the program Sparky 3 (T.D. Goddard and D.G. Kneller, University

Biochemical Journal (2017) **474** 2219–2233
DOI: 10.1042/BCJ20170173

of California, San Francisco) using the assignments determined from the solution structure of RNase 1 [52]. The vector changes of chemical shift ($\Delta\Delta\delta$) were determined with the following equation:

$$\Delta\Delta\delta = \sqrt{(\Delta\delta^{1}\mathrm{H})^{2} + \left(\frac{1}{5}\Delta\delta^{15}\mathrm{N}\right)^{2}} \quad (2)$$

where ^{1}H and ^{15}N chemical shifts ($\Delta\delta$) were the peak chemical shifts of [^{15}N]-RNase 1 in the presence minus the absence of HS or PS.

Sequence alignment and phylogenetic analyses

Protein sequence alignments were made with the program MUSCLE [53] with manual adjustments. A neighbor-joining phylogenetic tree based on amino acid sequences was generated in MEGA6 using the Jones–Taylor–Thornton (JTT) substitution model with a discrete Gamma (+G) distribution to model evolutionary rate differences among sites [54] and 1000 bootstrap replicates [55]. The evolutionary model (JTT+G) was inferred according to the Akaike Information Criterion statistics obtained with the jModelTest program run with the MEGA6 software.

The evolutionary rate of each site in the aligned amino acid sequences of 30 RNase 1 homologs [55] was also calculated with the MEGA6 software and the JTT+G evolutionary model (for a list of GenBank Accession numbers, see Supplementary Table S2). The calculated rates were scaled such that the average evolutionary rate across all sites was 1. Hence, sites with a rate of <1 are evolving slower than average, and sites with a rate of >1 are evolving faster than average. To visualize these evolutionary rates in the context of protein structure, an image of PDB entry 1z7× for human RNase 1 [56] was created with the program PyMOL (Schrödinger) in which the evolutionary rate of each residue was inserted as its β-factor.

Table 1 Steady-state kinetic parameters of homologous RNases

Species	pH optimum for ssRNA	k_{cat}/K_M (10^6 M^{-1} s^{-1}) for ssRNA at pH optimum[1]	k_{cat}/K_M (10^3 mM^{-1} min^{-1}) for poly(A:U) at pH 7.4[1]	k_{cat}/K_M (10^3 mM^{-1} min^{-1}) for poly(I:C) at pH 7.4[1]	Product (%) from hairpin at pH 7.4[2]
Human (*Homo sapiens*)	7.3	3 ± 1	12 ± 3	0.7 ± 0.2	89 ± 11
Bat (*M. lucifugus*)	7.3	3 ± 1	10 ± 3	0.5 ± 0.1	89 ± 6
Squirrel (*S. carolinensis*)	6.8	6 ± 1	3.4 ± 0.7	0.4 ± 0.1	54 ± 6
Horse (*Equus ferus caballus*)	6.5	8 ± 1	1.0 ± 0.2	0.4 ± 0.2	33 ± 4
Cat (*Felis catus*)	6.5	6.9 ± 0.1	0.023 ± 0.006	0.16 ± 0.08	24 ± 11
Mouse (*Mus musculus*)	6.4	8 ± 3	0.006 ± 0.002	0.05 ± 0.01	17 ± 2
Cow (*Bos taurus*)	6.1	13 ± 2	0.007 ± 0.002	0.04 ± 0.01	13 ± 3
Chicken (*Gallus gallus*)	6.2	0.7 ± 0.4	<0.001	<0.001	6 ± 2
Anole (*Anolis carolinensis*)	6.2	0.04 ± 0.01	<0.001	<0.001	5 ± 3
Frog (*Rana pipiens*)	6.2	0.03 ± 0.01	<0.001	<0.001	2 ± 2

[1]Values are the mean ± SD from 4 to 7 independent experiments.
[2]Values are the mean ± SD from 3 to 7 independent native gels like that in Supplementary Figure S3.

PORTLAND PRESS

Biochemical Journal (2017) 474 2219–2233
DOI: 10.1042/BCJ20170173

Results

For our analysis, we chose 10 RNase 1 homologs that span the vertebrate subphylum. These 10 include four mammalian homologs that had not been studied previously (bat, cat, horse, and squirrel). We cloned genes encoding these 10 RNases, expressed these genes in *Escherichia coli*, and purified the ensuing RNases to >99% purity (Supplementary Figure S1A). All of the RNase 1 homologs share a small size, net positive charge, and high thermostability (Supplementary Table S3). Additionally, we found that the four novel mammalian RNase 1 homologs used in the present study bind tightly to the mammalian RNase inhibitor protein (Supplementary Figure S1B), in accordance with homologs characterized previously [8,43].

RNase 1 homologs exhibit pronounced differences in catalysis

We sought to probe properties of enzymatic function. Previous studies have shown that homologous RNases can exhibit different pH optima for catalysis, and such differences can provide clues regarding biological localization and function [30,31]. We found similar distinctions. Using a small fluorogenic substrate that enables a continuous assay of single-stranded (ss)RNA hydrolysis, we established a pH–rate profile for each enzyme (Supplementary Figure S2). We found that cow RNase 1 manifested the highest catalytic activity, but did so at the lowest pH optimum (6.1). Other mammalian homologs demonstrated a range of increasingly lower enzymatic activities at increasingly higher pH optima. Human RNase 1 was at the opposite end of the spectrum from cow RNase 1, with ∼5-fold lower activity at a much higher optimal pH (7.3) (Table 1). Nonmammalian homologs (chicken, anole lizard, and frog) all demonstrated very low catalytic activity at relatively low pH.

Although all ptRNases can degrade ssRNA substrates, only a small subset display high activity toward dsRNA substrates [33]. Such a feature is consistent with a role in host defense, as antigenic dsRNAs can be produced or released by viruses and bacteria and are known to activate inflammatory responses [57]. We determined the ability of RNase 1 homologs to degrade poly(I:C) and poly(A:U), two synthetic analogs of viral RNA. Intriguingly, human, bat, squirrel, and horse homologs displayed a pronounced ability to degrade dsRNA. For poly(A:U), human and bat RNase 1 showed the highest activity, with catalytic efficiencies ∼1800-fold higher and ∼1400-fold higher, respectively, than that of cow RNase 1 (Table 1). Human RNase 1 demonstrated significantly higher activity than all other homologs, except for bat RNase 1. For poly(I:C), the trend was similar though less robust, with human RNase 1 showing ∼18-fold higher and bat RNase 1 showing ∼14-fold higher catalytic efficiency than did cow RNase 1 (Table 1). Cat RNase 1 was moderately active against both substrates, whereas cow and mouse RNase 1 exhibited the lowest activity of the mammalian homologs. These trends are in line with previous studies that probed the differential ability of RNase 1 homologs to degrade dsRNA [27,30,31,33]. The nonmammalian homologs showed no measureable activity against either dsRNA substrate (Table 1). The catalytically inactive H12A variant of human RNase 1 was used as a negative control and did not exhibit detectable activity against either substrate.

To confirm that the measured activity was specific for a dsRNA substrate—and not confounded by the potentially heterogeneous nature of poly(A:U) and poly(I:C)—we employed an RNA/DNA hairpin substrate that contains a single ribonucleotide embedded within the sequence of a DNA oligonucleotide and that is labeled on the 5′-end with a fluorophore. We monitored the formation of the fluorescent 6-mer cleavage product of RNase catalysis by electrophoresis using a native polyacrylamide gel (Supplementary Figure S3). Densitometric analysis of substrate and cleavage products mirrored the same trend observed with the poly(A:U) and poly(I:C) substrates. Specifically, human and bat RNase 1 demonstrated the most product formation (∼90% for both) followed by squirrel RNase 1 (∼54%) and then the enzymes from horse, cat, mouse, and cow (Table 1). Again, human RNase 1 showed significantly higher activity than did other homologs, with the exception of bat RNase 1. As with the previous dsRNA substrates, H12A human RNase 1 and the nonmammalian homologs demonstrated negligible activity.

RNase 1 orthologs differ in their cellular entry and affinity for cell-surface components

RNase 1 homologs can enter human cells via endosomal translocation, a surprising trait that might be related to endogenous function. The association of RNase 1 with cell-surface glycans could aid this process [44,50]. We were curious to know if the enzymes in our study have a similar ability to enter cells, and if this ability correlates with affinity for cell-surface moieties.

Biochemical Journal (2017) **474** 2219–2233
DOI: 10.1042/BCJ20170173

We measured the cellular uptake of fluorophore-labeled RNase 1 homologs by a non-adherent human cell line (K-562) using flow cytometry. Interestingly, we found that all of the proteins in our study, both mammalian and nonmammalian, were taken up readily by cells (Figure 1A). Of the mammalian orthologs, human RNase 1 demonstrated the highest level of cellular internalization, followed by bat and squirrel RNase 1. Anole RNase 1 was internalized similarly to human RNase, with chicken RNase also showing appreciable internalization. Cow and frog RNase showed the lowest levels of internalization.

We hypothesized that those RNase orthologs with the highest levels of cellular uptake might bind more tightly to cell-surface glycans. We used fluorescence polarization to determine the affinities of fluorophore-labeled RNase 1 homologs for common cell-surface glycosaminoglycans, including HS (approximated with heparin in our study; Supplementary Figure S4), as well as two forms of chondroitin sulfate. We found that the observed trend in cellular uptake of mammalian RNase 1 homologs was mirrored by their affinity for glycans: human and bat RNase 1 showed extremely tight (nanomolar) affinity for each glycan, and squirrel RNase 1 demonstrated moderately tight glycan binding (Figure 1). Of the mammalian proteins, cow and mouse RNase 1 exhibited the weakest binding, mirroring their lower levels of cellular uptake. For the nonmammalian orthologs, however, cellular uptake did not match glycan binding. Indeed, all of the nonmammalian homologs showed weak and, perhaps, physiologically irrelevant affinity for cell-surface glycans (Figure 1). These results are consistent with the uptake of nonmammalian homologs relying more on overall cationicity than on specific interactions with cell-surface components [46].

To provide high resolution on the binding of human RNase 1 to cell-surface moieties, we employed ^{1}H,^{15}N-HSQC NMR spectroscopy [51] to identify those residues in the human enzyme that interact with HS and PS, two prevalent membrane components. The backbone ^{1}H and ^{15}N NMR assignments for human RNase 1 were determined previously [52]. We found that the presence of zwitterionic CTAB micelles elicited few changes in the ^{1}H and ^{15}N chemical shifts. In contrast, these shifts were perturbed markedly by micelles containing an HS mimic or PS at one molar equivalent relative to RNase 1 (Figure 2). Major shift perturbations for both HS and PS were found throughout the amino acid sequence, with large perturbations clustered predominantly to a polar serine-rich loop, Ser18–Thr24, as well as at Cys72, Asn76, and His80.

Rapidly evolving RNase 1 residues are associated with novel functions

Mammalian RNase 1 orthologs share a high degree of identity and similarity in their amino acid sequences (Supplementary Table S4). Still, due to the significant functional differences uncovered in our study, we were

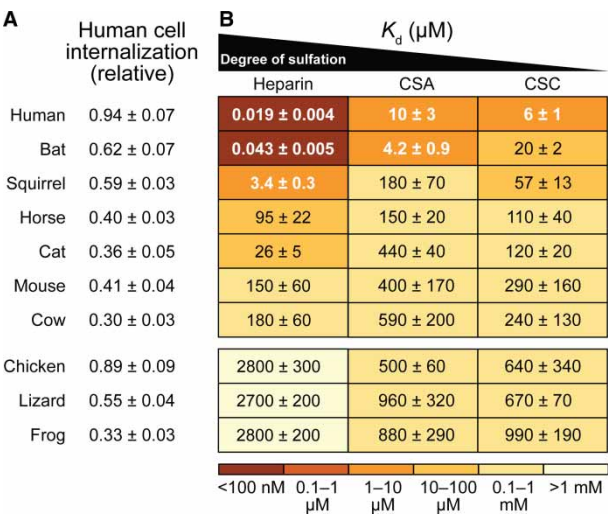

Figure 1. Cellular binding and entry.

(**A**) Values of relative fluorescence for K-562 cells treated with an RNase 1–BODIPY conjugate (5 μM) for 4 h and then washed twice with PBS. Values are the mean ± SEM from five to nine independent flow cytometry experiments. (**B**) Values of K_d (μM) for the complex of RNase 1–BODIPY conjugates and cell-surface glycosaminoglycans, which have different levels of sulfation. Values are the mean ± SEM from three to six independent fluorescence polarization experiments, and are overlaid on a heatmap depicting relative affinity. CSA, chondroitin sulfate A; CSC, chondroitin sulfate C.

Biochemical Journal (2017) **474** 2219–2233
DOI: 10.1042/BCJ20170173

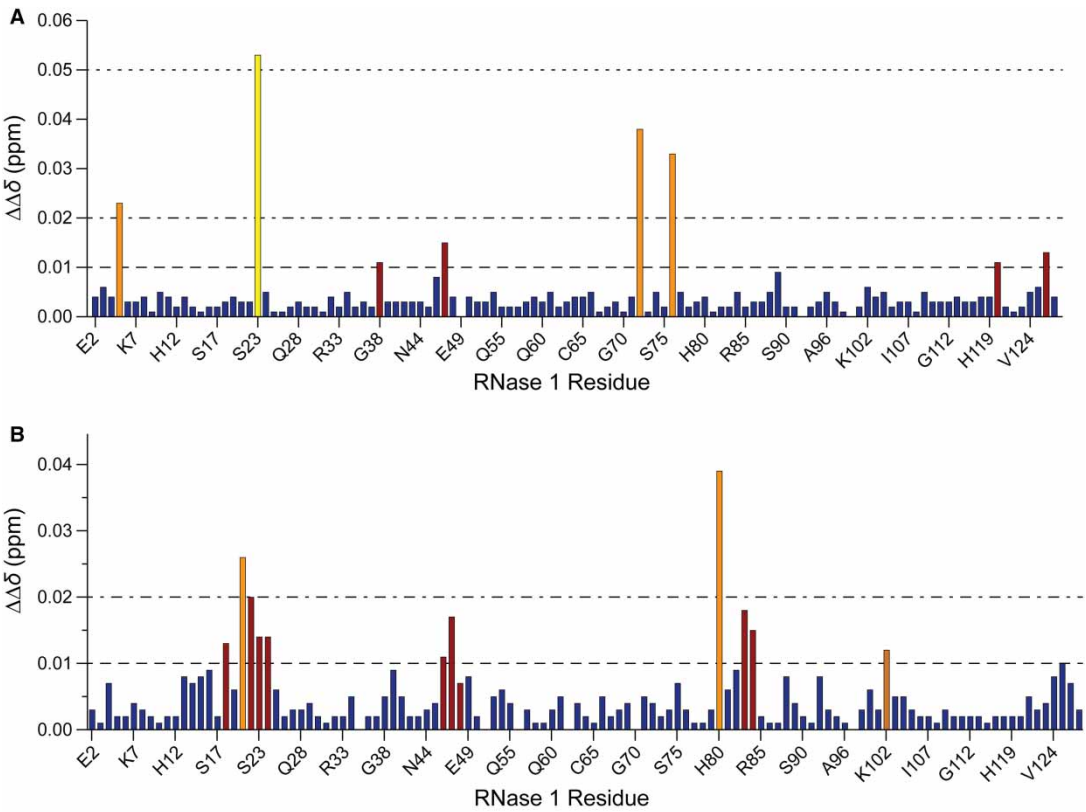

C

Interactions between human RNase 1 and cell-surface ligands

Cell-surface ligand	ΔΔδ (ppm)	Perturbed residues
Heparan sulfate	>0.01	G38, V47, F120, D126
	>0.02	A4, C72, N76
	>0.05	S23
Phosphatidylserine	>0.01	S18, S22, S23, T24, F46, V47, D83, C84, K102
	>0.02	S21, H80

Figure 2. Interaction of human RNase 1 with cell-surface ligands.

(**A** and **B**) Bar graphs of perturbations to the NMR chemical shifts of human [^{15}N]-RNase 1 induced by a cell-surface ligand. A solution of human [^{15}N]-RNase 1 was incubated with CTAB micelles that contained a molar equivalent of a mimic of HS (**A**) or phosphatidylserine (**B**). (**C**) List of human RNase 1 residues that had the largest perturbations induced by a mimic of HS or phosphatidylserine.

curious to know if certain regions of the proteins were changing more quickly over time. We aligned the protein sequences of 30 mammalian RNase 1 homologs and used the program MEGA6 to estimate the mean (relative) evolutionary rate for each amino acid position. To visualize the relative evolutionary rates of specific residues in the context of protein structure, we created an image of human RNase 1 in which values of relative evolutionary rate were inserted as the β-factor for each atom (Figure 3A). We found that the majority of rapidly evolving residues were on the protein surface, whereas many residues considered integral for protein structure, as well as for enzymatic activity, were highly conserved across species.

We also linearly mapped the relative evolutionary rates as a heatmap corresponding to a protein sequence alignment for the various RNase 1 homologs used in our study (Figure 3B). Previous structure–function analyses of RNase 1 variants have identified amino acid residues predicted to be involved in a variety of functions, including residues involved in the cleavage of ssRNA [10,58,59], residues associated with the degradation of dsRNA [27,60,61], and residues involved in binding to the RNase inhibitor [56]. We found a dramatic correlation between residues predicted to be evolving faster and those residues associated with

Biochemical Journal (2017) **474** 2219–2233
DOI: 10.1042/BCJ20170173

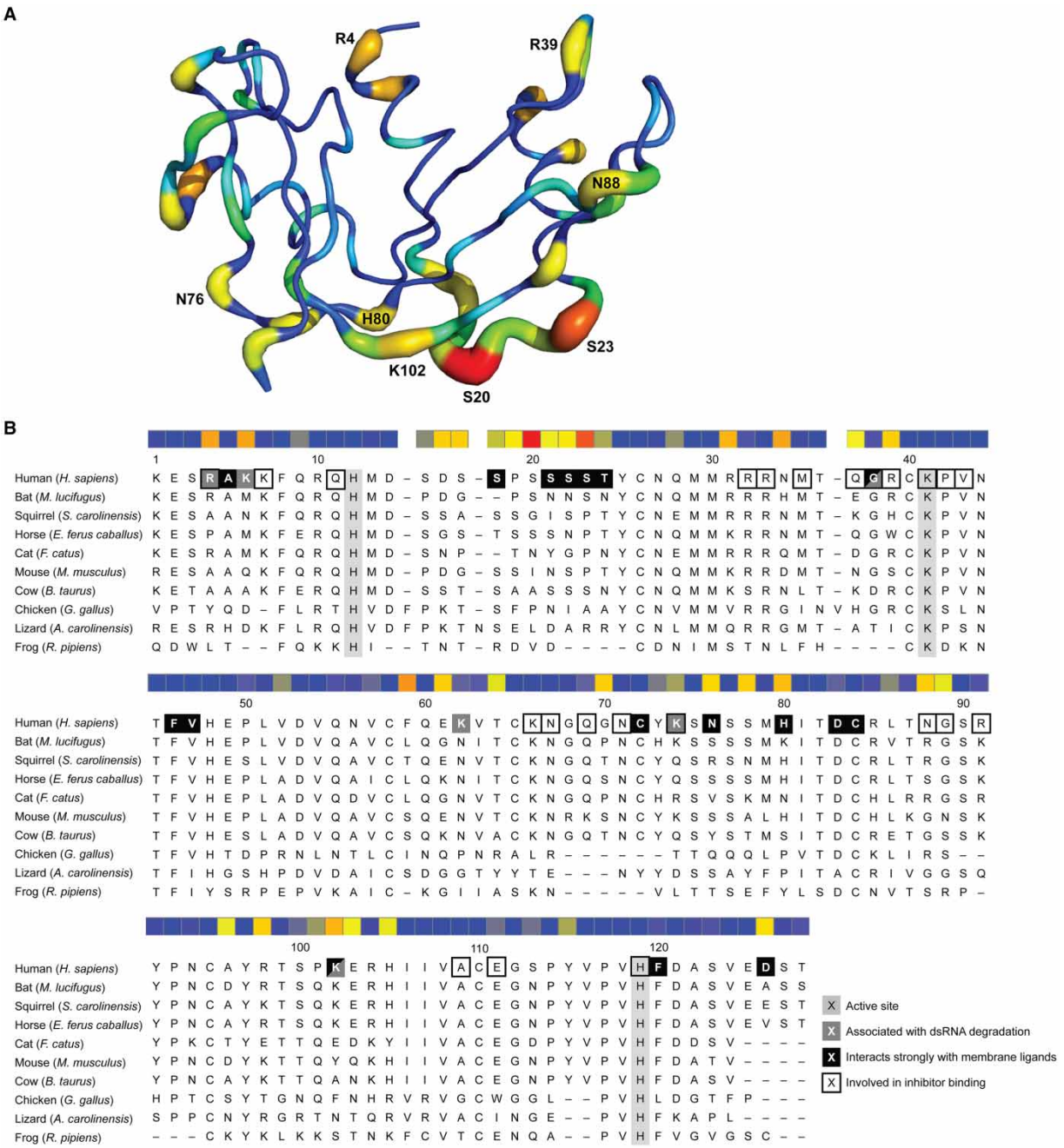

Figure 3. Predicted evolution of RNase 1 enzymes.

(**A**) Three-dimensional structure of human RNase 1 in which residues predicted to be evolving at a faster rate are depicted with both a thicker backbone and a hotter color (red > orange > yellow > green > aqua > blue). The eight residues predicted to be evolving at the fastest rate are labeled explicitly. (**B**) Protein sequence alignment for the 10 RNase 1 homologs used in the present study. A heatmap in which the predicted evolutionary rates of residues is depicted with colors as in **A**. The three key active-site residues are highlighted in light gray; residues in human RNase 1 known to correspond to various functions are labeled as indicated in the legend. Asn34, Asn76, and Asn88 in human RNase 1 are known to be *N*-glycosylated.

properties such as dsRNA degradation (e.g. Arg4, Lys6, and Lys102) and cell-surface binding (e.g. Ser21, Ser22, Ser 23, Asn76, and His80). We note also that asparagine residues that can undergo *N*-linked glycosylation prior to protein secretion were also predicted to be rapidly evolving sites (Asn34, Asn76, and Asn88). The

Biochemical Journal (2017) **474** 2219–2233
DOI: 10.1042/BCJ20170173

recombinant proteins in our study lacked *N*-glycosylation, which could have effects on their function in their native environment.

Interestingly, we found that the key residues in the enzymic active site (His12, Lys41, and His119), along with those required for binding to an RNase inhibitor (including Lys7, Arg33, Met35, Pro42, Val43, Lys66, Asn71, Ala109, and Glu111), are generally conserved across species, consistent with stabilizing selection to retain these properties in all homologs.

Discussion

RNase 1 is an efficacious ribonucleolytic enzyme that circulates freely through biological fluids in all vertebrate animals. Despite its evolutionary conservation and robust presence *in vivo*, the physiological role of this enzyme is only beginning to be appreciated fully. To narrow this deficit, we have performed a comparative functional analysis of RNase 1 homologs from a broad subset of species, representing six orders of eutherian mammals, as well as the avian, reptilian, and amphibian classes. This analysis, which is the first to quantify relevant biochemical properties of a large variety of homologous vertebrate RNases, reveals pronounced functional differences not only between mammalian and nonmammalian proteins, but also between proteins from various mammalian species. We have uncovered differences in catalytic activity against both single-stranded and double-stranded RNA, as well as differential pH optima for maximum catalytic efficiency. We have also observed that certain RNase 1 homologs can enter cells much more readily than others, and that this ability correlates with enhanced cell-surface binding. Taken together, our functional characterization adds further evidence to the supposition that, apart from specially evolved variants of RNase 1 that exist in ruminant animals, the broader physiological role of RNase 1 has little to do with digestion.

We uncovered stark differences between the characteristics of mammalian versus nonmammalian RNase 1 homologs, which could illuminate the origins of the ptRNase family. Interestingly, ptRNases have been found only in vertebrates, and database searches against the genomes of invertebrates such as flies, worms, and ascidians did not yield any significant matches [4]. Nonetheless, ptRNase family members have been identified in a host of amphibian, avian, reptilian, and fish species, and select members of these groups have been found to have novel properties. For example, nonmammalian ptRNases display much lower ribonucleolytic activity against ssRNA substrates [62,63]. Yet, several nonmammalian enzymes possess antimicrobial and angiogenic properties [64–66]. These properties are notable because RNase 5, also known as angiogenin, is a prominent and well-studied mammalian ptRNase. Angiogenin is known to promote angiogenesis, has demonstrated antimicrobial activity and other functions [67–69], and operates by a unique mechanism [70]. Like the nonmammalian RNases in our study, human angiogenin exhibits extremely low catalytic activity against ssRNA substrates and virtually no activity against dsRNA substrates (data not shown). Correspondingly, large-scale phylogenetic analyses of many nonmammalian and mammalian ptRNases indicate that the nonmammalian homologs are most evolutionarily similar to angiogenin, predicting a common ancestral enzyme [4]. Given the shared attributes of many nonmammalian ptRNases to the mammalian angiogenins, it is likely that RNase 5 represents the most ancient form of the mammalian enzyme, and that all other members arose from RNase 5 during mammalian evolution. An intriguing hypothesis is that the superfamily originated as a host-defense/pro-growth mechanism during early vertebrate evolution and underwent massive functional expansion in mammals, resulting in the current diversity of the family. The number of ptRNase genes in mammals is quite large (typically, 13–20), whereas avian and amphibian species lack such diversity [4]. This coincides with adaptive radiation of mammalian diversity occurring during the Cenozoic era.

Our data indicate that various RNase 1 homologs have optimal activity at vastly different pHs. For example, cow RNase 1 (i.e. RNase A) was the most active enzyme against ssRNA at the lowest pH. These results align well with the observation that RNase A is secreted in abundance from the bovine exocrine pancreas into the rumen, which is a harsh environment with a normal pH range of 5.8–6.4. There, RNase A is believed to degrade mRNA from symbiotic bacteria to assist with foregut fermentation and digestion [23]. Yet, we found that in nonruminant animals, there is a distinct shift in pH optima. For example, human and bat RNase 1 enzymes have a pH optimum of 7.3, which is indistinguishable from the pH of many human biological fluids, including blood (pH 7.4). These findings suggest that, aside from digestion-specific homologs in ruminants, mammalian RNase 1 has adapted to circulate widely *in vivo* and to operate outside of the digestive tract.

A striking finding from our study was the different ability of various homologs to degrade dsRNA. We found that the ptRNases from human and bat had the highest activity by a large margin (Table 1 and Figure 4). Degradation of dsRNA could have profound implications *in vivo*. Recent work has identified

Biochemical Journal (2017) **474** 2219–2233
DOI: 10.1042/BCJ20170173

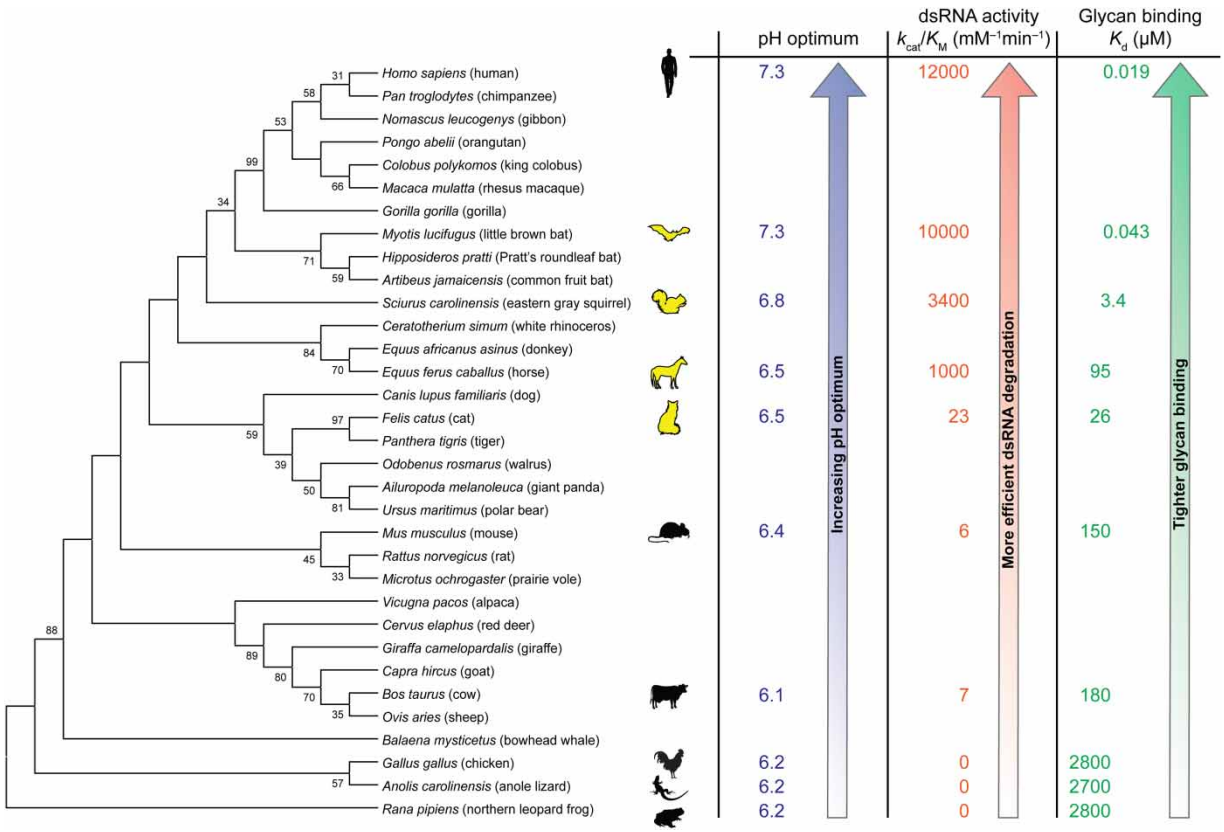

Figure 4. Schematic summary of the diverse function of RNase 1 homologs across an evolutionary spectrum.
A neighbor-joining phylogenetic tree shows the evolutionary relationship of homologous RNases (bootstrap values >30 are shown). Functional data obtained from the present study, including the pH optimum for catalysis, ability to catalyze the cleavage of a dsRNA [poly(A:U)], and affinity for a glycan (heparin), are mapped onto the tree and indicate an increasingly refined phenotype for the human homolog. The RNase 1 homologs from bat, squirrel, horse, and cat (yellow) had not been characterized previously and fill a large gap between the human and mouse enzymes.

extracellular RNA (exRNA) as a heterogeneous class of secreted cofactors in bodily fluids that can contribute to coagulation, blood vessel permeability, cell–cell signaling, tumor progression, and inflammation. They can be ss- or ds, and can originate from internal cells or from antigenic sources, such as invading bacteria or viruses [71,72]. As the only known RNase in bodily fluids with high, nonspecific ribonucleolytic activity, RNase 1 might be a natural regulator of exRNA. Additionally, exRNAs are recognized by Toll-like receptors 3, 7, and 8, which are expressed inside the endosomes of endothelial and immune cells [73]. Significantly, we found that some mammalian RNase 1 homologs not only degrade dsRNA efficiently, but also enter endosomes readily, potentially mediated by interactions with cell-surface glycans. Human RNase 1, in particular, might be especially well adapted to degrade antigenic exRNA both within endosomes and in the extracellular space, suggesting an important role for human RNase 1 in regulating processes like coagulation and inflammation [72]. The amino acid sequence of human RNase 1 is identical with that of the Neanderthal enzyme [74], indicative of its biological role being established in a common ancestor at least 550 000 years ago.

Remarkably, many of the key residues that are predicted to be important for RNase 1 function—including dsRNA digestion and binding to cell-surface moieties—appear to be evolving at a faster rate than other residues (Figure 3). Not surprisingly, the most conserved residues across vertebrate RNase 1 homologs appear to be those involved in the catalytic active site, as well as those involved with binding to an RNase inhibitor, suggesting that such properties have been maintained throughout diversification. Taken together, our findings indicate that although the core structure and function of RNase 1 has remained consistent throughout evolution, the adaptation of various surface residues has contributed to distinct functional differences across species.

Biochemical Journal (2017) **474** 2219–2233
DOI: 10.1042/BCJ20170173

Moreover, our study underscores the notion that a few changes to surface residues can manifest as markedly different biochemical and physiological properties.

Some of the functional data herein were predicted by previous studies in molecular genetics. Using phylogenetic analysis, Rosenberg and co-workers demonstrated that squirrel *RNase1* genes emerged as a distinct cluster apart from *RNase1* genes from mouse or rat [35]. They also predicted that some distinct surface substitutions might be impactful for biological function. Our results show that the biochemical properties of squirrel RNase 1 are indeed different from those of mouse RNase 1, and the squirrel enzyme appears to function more similarly to human or bat RNase 1 than to the rodent enzyme. Yu and Zhang [75] analyzed *RNase1* genes across a large spectrum of carnivores and detected positive selection toward greater cationicity, suggesting the onset of novel functional adaptations not related to digestion. Similarly, our study found that cat RNase 1 possesses distinct properties from digestion-specific RNase A. Zhang and co-workers screened for the *RNase1* gene in more than 20 bat species and detected evidence of adaptive gene duplication events that did not correlate to feeding habits. Their work, along with analyses by Goo and Cho, highlighted the rapid expansion of *RNase1* genes in bat species, suggesting that RNase 1 might play other roles in bats unrelated to digestion [6,36]. Our work supports this hypothesis, as we found that bat RNase 1 displays markedly different properties from RNase A, and is indeed much more similar to human RNase 1 than to any other homolog. We note, however, that the version of bat RNase 1 tested in our current study represents only a single version of many paralogous *RNase1* genes found in the little brown bat genome [6].

Another ongoing mystery is how *N*-glycosylation of RNase 1 influences or regulates its endogenous function. Residues in human RNase 1 that undergo N-linked glycoslyation are evolving more quickly than other residues (Figure 3). Analyses of human tissues and fluids indicate that various sources produce differentially glycosylated forms of RNase 1 [76,77]. Differences in the function of these variously glycosylated forms of RNase 1 are not clear, though one hypothesis is that heavily glycosylated RNase 1 might be able to evade the RNase inhibitor, serving as a natural mimic of the engineered form of RNase 1 currently in clinical trials for various types of cancer [21,22]. Support for this hypothesis comes from recent data that showed a significant increase in the serum levels of RNase 1 containing *N*-glycosylated Asn88 in patients with pancreatic cancer [78]. In effect, the glycosylation of RNase 1 could constitute an unappreciated natural anticancer mechanism.

Proteins are subjected to natural selection as a result of evolutionary pressures on the organisms that contain them. As novel attributes often evolve incrementally, comparative functional analyses of a protein in related species can yield an enhanced understanding of biology and physiology [38–41]. From our data, we speculate that RNase 1 in humans and other mammals serves a broad regulatory role via the degradation of serum RNA, potentially mediating critical processes such as hemostasis, inflammation, and innate immunity (including anticancer activity).

Abbreviations

CTAB, cetyltrimethylammonium bromide; ds, double stranded; DSF, differential scanning fluorimetry; exRNA, extracellular RNA; HS, heparan sulfate; MES, 2-(*N*-morpholino)ethanesulfonic acid; PS, phosphatidylserine; ptRNases, pancreatic-type ribonucleases; RI, RNase inhibitor; RNase 1, ribonuclease 1; ss, single stranded.

Author Contribution

J.E.L. and C.H.E. conceived the project, performed experiments, and acquired the data. All authors analyzed and interpreted the data, and wrote the manuscript.

Funding

J.E.L. was supported by an National Science Foundation Graduate Research Fellowship. This work was supported by Grant R01 CA073808 (National Institutes of Health, NIH), and made use of the National Magnetic Resonance Facility at Madison, which was supported by Grant P41 GM103399 (NIH).

Acknowledgements

We are grateful to Dr David S. Blehert, and Elizabeth A. Bohuski of the USGS National Wildlife Health Center (Madison, WI, U.S.A.) for providing little brown bat tissue; Dr Angela J. Gruber, Benjamin W. Gruber, and Emily R. Garnett (University of Wisconsin-Madison) for providing squirrel tissue; Drs W. Milo Westler and Marco Tonelli (University of Wisconsin-Madison) for advice with HSQC NMR spectroscopy; and Dr Trish T. Hoang for contributive discussions.

PORTLAND PRESS

Competing Interests

The authors declare the following competing financial interest(s): R.T.R. is a founder of Quintessence Biosciences, Inc. (Madison, WI), which is developing cancer chemotherapeutic agents based on ribonucleases.

References

1 Sorrentino, S. (2010) The eight human 'canonical' ribonucleases: molecular diversity, catalytic properties, and special biological actions of the enzyme proteins. *FEBS Lett.* **584**, 2194–2200 doi:10.1016/j.febslet.2010.04.018
2 Koczera, P., Martin, L., Marx, G. and Schuerholz, T. (2016) The ribonuclease A superfamily in humans: canonical RNases as the buttress of innate immunity. *Int. J. Mol. Sci.* **17**, 1278 doi:10.3390/ijms17081278
3 Beintema, J.J., Breukelman, H.J., Carsana, A. and Furia, A. (1997) Evolution of vertebrate ribonucleases: ribonuclease A superfamily. In *Ribonucleases: Structures and Functions* (D'Alessio, G. and Riordan, J.F., eds), pp. 245–269, Academic Press, New York
4 Cho, S., Beintema, J.J. and Zhang, J. (2005) The ribonuclease A superfamily of mammals and birds: identifying new members and tracing evolutionary histories. *Genomics* **85**, 208–220 doi:10.1016/j.ygeno.2004.10.008
5 Dyer, K.D. and Rosenberg, H.F. (2006) The RNase A superfamily: generation of diversity and innate host defense. *Mol. Divers.* **10**, 585–597 doi:10.1007/s11030-006-9028-2
6 Goo, S.M. and Cho, S. (2013) The expansion and functional diversification of the mammalian ribonuclease A superfamily epitomizes the efficiency of multigene families at generating biological novelty. *Genome Biol. Evol.* **5**, 2124–2140 doi:10.1093/gbe/evt161
7 Dickson, K.A., Haigis, M.C. and Raines, R.T. (2005) Ribonuclease inhibitor: structure and function. *Prog. Nucleic Acid Res. Mol. Biol.* **80**, 349–374 doi:10.1016/S0079-6603(05)80009-1
8 Lomax, J.E., Bianchetti, C.M., Chang, A., Phillips, Jr, G.N., Fox, B.G. and Raines, R.T. (2014) Functional evolution of ribonuclease inhibitor: insights from birds and reptiles. *J. Mol. Biol.* **426**, 3041–3056 doi:10.1016/j.jmb.2014.06.007
9 D'Alessio, G. and Riordan, J.F. (eds) (1997) *Ribonucleases: Structures and Functions.* Academic Press, New York
10 Raines, R.T. (1998) Ribonuclease A. *Chem. Rev.* **98**, 1045–1066 doi:10.1021/cr960427h
11 Marshall, G.R., Feng, J.A. and Kuster, D.J. (2008) Back to the future: ribonuclease A. *Biopolymers* **90**, 259–277 doi:10.1002/bip.20845
12 Su, A.I., Wiltshire, T., Batalov, S., Lapp, H., Ching, K.A., Block, D. et al. (2004) A gene atlas of the mouse and human protein-encoding transcriptomes. *Proc. Natl Acad. Sci. U.S.A.* **101**, 6062–6067 doi:10.1073/pnas.0400782101
13 Morita, T., Niwata, Y., Ohgi, K., Ogawa, M. and Irie, M. (1986) Distribution of two urinary ribonuclease-like enzymes in human organs and body fluids. *J. Biochem.* **99**, 17–25 doi:10.1093/oxfordjournals.jbchem.a135456
14 Kurihara, M., Ogawa, M., Ohta, T., Kurokawa, K. and Kitahara, T. (1982) Purification and immunological characterization of human pancreatic ribonuclease. *Cancer Res.* **42**, 4836–4841 PMID:6812951
15 Beintema, J.J., Wietzes, P., Weickmann, J.L. and Glitz, D.G. (1984) The amino acid sequence of human pancreatic ribonuclease. *Anal. Biochem.* **136**, 48–64 doi:10.1016/0003-2697(84)90306-3
16 Weickmann, J.L., Olson, E.M. and Glitz, D.G. (1984) Immunological assay of pancreatic ribonuclease in serum as an indicator of pancreatic cancer. *Cancer Res.* **44**, 1682–1687 PMID:6704974
17 Fischer, S., Nishio, M., Dadkhahi, S., Gansler, J., Saffarzadeh, M., Shibamiyama, A. et al. (2011) Expression and localisation of vascular ribonucleases in endothelial cells. *Thromb. Haemost.* **105**, 345–355 doi:10.1160/TH10-06-0345
18 Leland, P.A. and Raines, R.T. (2001) Cancer chemotherapy — ribonucleases to the rescue. *Chem. Biol.* **8**, 405–413 doi:10.1016/S1074-5521(01)00030-8
19 Benito, A., Ribó, M. and Vilanova, M. (2005) On the track of antitumour ribonucleases. *Mol. BioSyst.* **1**, 294–302 doi:10.1039/b502847g
20 Lee, J.E. and Raines, R.T. (2008) Ribonucleases as novel chemotherapeutics: the ranpirnase example. *BioDrugs* **22**, 53–58 doi:10.2165/00063030-200822010-00006
21 Strong, L.E., Kink, J.A., Pensinger, D., Mei, B., Shahan, M. and Raines, R.T. (2012) Abstract 1838: efficacy of ribonuclease QBI-139 in combination with standard of care therapies. *Cancer Res.* **72**(Suppl 8), 1838 doi:10.1158/1538-7445.AM2012-1838
22 Strong, L.E., Kink, J.A., Mei, B., Shahan, M.N. and Raines, R.T. (2012) First in human phase I clinical trial of QBI-139, a human ribonuclease variant, in solid tumors. *J. Clin. Oncol.* **30**(Suppl.), TPS3113
23 Barnard, E.A. (1969) Biological function of pancreatic ribonuclease. *Nature* **221**, 340–344 doi:10.1038/221340a0
24 Snook, J.T. (1965) Dietary regulation of pancreatic enzyme synthesis, secretion and inactivation in the rat. *J. Nutr.* **87**, 297–305 PMID:5859256
25 Peterson, L.M. (1979) Serum RNase in the diagnosis of pancreatic carcinoma. *Proc. Natl Acad. Sci. U.S.A.* **76**, 2630–2634 doi:10.1073/pnas.76.6.2630
26 Schein, C.H. (1997) From housekeeper to microsurgeon: the diagnostic and therapeutic potential of ribonucleases. *Nat. Biotechnol.* **15**, 529–536 doi:10.1038/nbt0697-529
27 Jermann, T.M., Opitz, J.G., Stackhouse, J. and Benner, S.A. (1995) Reconstructing the evolutionary history of the artiodactyl ribonuclease superfamily. *Nature* **374**, 57–59 doi:10.1038/374057a0
28 Beintema, J.J. and Benner, S.A. (2002) Ribonucleases in ruminants. *Science* **297**, 1121–1122 doi:10.1126/science.297.5584.1121b
29 Antignani, A., Naddeo, M., Cubellis, M.V., Russo, A. and D'Alessio, G. (2001) Antitumor action of seminal ribonuclease, its dimeric structure, and its resistance to the cytosolic ribonuclease inhibitor. *Biochemistry* **40**, 3492–3496 doi:10.1021/bi002781m
30 Eller, C.H., Lomax, J.E. and Raines, R.T. (2014) Bovine brain ribonuclease is the functional homolog of human ribonuclease 1. *J. Biol. Chem.* **289**, 25996–26006 doi:10.1074/jbc.M114.566166
31 Zhang, J., Zhang, Y.-p. and Rosenberg, H.F. (2002) Adaptive evolution of a duplicated pancreatic ribonuclease gene in a leaf-eating monkey. *Nat. Genet.* **30**, 411–415 doi:10.1038/ng852
32 Wang, Z., Xu, S., Du, K., Huang, F., Chen, Z., Zhou, K. et al. (2016) Evolution of digestive enzymes and RNASE1 provides insights into dietary switch of cetaceans. *Mol. Biol. Evol.* **33**, 3144–3157 doi:10.1093/molbev/msw191

Biochemical Journal (2017) **474** 2219–2233
DOI: 10.1042/BCJ20170173

33 Libonati, M. and Sorrentino, S. (2001) Degradation of double-stranded RNA by mammalian pancreatic-type ribonucleases. *Methods Enzymol.* **341**, 234–248 doi:10.1016/S0076-6879(01)41155-4

34 Dubois, J.-Y. F., Jekel, P.A., Mulder, P.P.M.F.A., Bussink, A.P., Catzeflis, F.M., Carsana, A. et al. (2002) Pancreatic-type ribonuclease 1 gene duplications in rat species. *J. Mol. Evol.* **55**, 522–533 doi:10.1007/s00239-002-2347-8

35 Siegel, S.J., Percopo, C.M., Dyer, K.D., Zhao, W., Roth, V.L., Mercer, J.M. et al. (2009) RNase 1 genes from the family Sciuridae define a novel rodent ribonuclease cluster. *Mamm. Genome* **20**, 749–757 doi:10.1007/s00335-009-9215-4

36 Xu, H., Liu, Y., Meng, F., He, B., Han, N., Li, G. et al. (2013) Multiple bursts of pancreatic ribonuclease gene duplication in insect-eating bats. *Gene* **526**, 112–117 doi:10.1016/j.gene.2013.04.035

37 Liu, J., Wang, X.-p., Cho, S., Lim, B.K., Irwin, D.M., Ryder, O.A. et al. (2015) Evolutionary and functional novelty of pancreatic ribonuclease: a study of Musteloidea (order Carnivora). *Sci. Rep.* **4**, 5070 doi:10.1038/srep05070

38 Dean, A.M. and Thornton, J.W. (2007) Mechanistic approaches to the study of evolution: the functional synthesis. *Nat. Rev. Genet.* **8**, 675–688 doi:10.1038/nrg2160

39 Soskine, M. and Tawfik, D.S. (2010) Mutational effects and the evolution of new protein functions. *Nat. Rev. Genet.* **11**, 572–582 doi:10.1038/nrg2808

40 Liberles, D.A., Teichmann, S.A., Bahar, I., Bastolla, U., Bloom, J., Bornberg-Bauer, E. et al. (2012) The interface of protein structure, protein biophysics, and molecular evolution. *Protein Sci.* **21**, 769–785 doi:10.1002/pro.2071

41 Harms, M.J. and Thornton, J.W. (2013) Evolutionary biochemistry: revealing the historical and physical causes of protein properties. *Nat. Rev. Genet.* **14**, 559–571 doi:10.1038/nrg3540

42 Smith, B.D., Soellner, M.B. and Raines, R.T. (2003) Potent inhibition of ribonuclease A by oligo(vinylsulfonic acid). *J. Biol. Chem.* **278**, 20934–20938 doi:10.1074/jbc.M301852200

43 Johnson, R.J., Lavis, L.D. and Raines, R.T. (2007) Intraspecies regulation of ribonucleolytic activity. *Biochemistry* **46**, 13131–13140 doi:10.1021/bi701521q

44 Chao, T.-Y., Lavis, L.D. and Raines, R.T. (2010) Cellular uptake of ribonuclease A relies on anionic glycans. *Biochemistry* **49**, 10666–10673 doi:10.1021/bi1013485

45 Lomax, J.E., Eller, C.H. and Raines, R.T. (2012) Rational design and evaluation of mammalian ribonuclease cytotoxins. *Methods Enzymol.* **502**, 273–290 doi:10.1016/B978-0-12-416039-2.00014-8

46 Sundlass, N.K., Eller, C.H., Cui, Q. and Raines, R.T. (2013) Contribution of electrostatics to the binding of pancreatic-type ribonucleases to membranes. *Biochemistry* **52**, 6304–6312 doi:10.1021/bi400619m

47 Niesen, F.H., Berglund, H. and Vedadi, M. (2007) The use of differential scanning fluorimetry to detect ligand interactions that promote protein stability. *Nat. Protoc.* **2**, 2212–2221 doi:10.1038/nprot.2007.321

48 Menzen, T. and Friess, W. (2013) High-throughput melting-temperature analysis of a monoclonal antibody by differential scanning fluorimetry in the presence of surfactants. *J. Pharm. Sci.* **102**, 415–428 doi:10.1002/jps.23405

49 Kelemen, B.R., Klink, T.A., Behike, M.A., Eubanks, S.R., Leland, P.A. and Raines, R.T. (1999) Hypersensitive substrate for ribonucleases. *Nucleic Acids Res.* **27**, 3696–3701 doi:10.1093/nar/27.18.3696

50 Eller, C.H., Chao, T.-Y., Singarapu, K.K., Ouerfelli, O., Yang, G., Markley, J.L. et al. (2015) Human cancer antigen Globo H Is a cell-surface ligand for human ribonuclease 1. *ACS Cent. Sci.* **1**, 181–190 doi:10.1021/acscentsci.5b00164

51 Ziarek, J.J., Peterson, F.C., Lytle, B.L. and Volkman, B.F. (2011) Binding site identification and structure determination of protein–ligand complexes by NMR: a semiautomated approach. *Methods Enzymol.* **493**, 241–275 doi:10.1016/B978-0-12-381274-2.00010-8

52 Kövér, K.E., Bruix, M., Santoro, J., Batta, G., Laurents, D.V. and Rico, M. (2008) The solution structure and dynamics of human pancreatic ribonuclease determined by NMR spectroscopy provide insight into its remarkable biological activities and inhibition. *J. Mol. Biol.* **379**, 953–965 doi:10.1016/j.jmb.2008.04.042

53 Edgar, R.C. (2004) MUSCLE: multiple sequence alignment with high accuracy and high throughput. *Nucleic Acids Res.* **32**, 1792–1797 doi:10.1093/nar/gkh340

54 Jones, D.T., Taylor, W.R. and Thornton, J.M. (1992) The rapid generation of mutation data matrices from protein sequences. *Comput. Appl. Biosci.* **8**, 275–282 PMID:1633570

55 Tamura, K., Stecher, G., Peterson, D., Filipski, A. and Kumar, S. (2013) MEGA6: Molecular Evolutionary Genetics Analysis version 6.0. *Mol. Biol. Evol.* **30**, 2725–2729 doi:10.1093/molbev/mst197

56 Johnson, R.J., McCoy, J.G., Bingman, C.A., Phillips, Jr, G.N. and Raines, R.T. (2007) Inhibition of human pancreatic ribonuclease by the human ribonuclease inhibitor protein. *J. Mol. Biol.* **368**, 434–449 doi:10.1016/j.jmb.2007.02.005

57 Tatematsu, M., Seya, T. and Matsumoto, M. (2014) Beyond dsRNA: Toll-like receptor 3 signalling in RNA-induced immune responses. *Biochem. J.* **458**, 195–201 doi:10.1042/BJ20131492

58 Findlay, D., Herries, D.G., Mathias, A.P., Rabin, B.R. and Ross, C.A. (1961) The active site and mechanism of action of bovine pancreatic ribonuclease. *Nature* **190**, 781–784 doi:10.1038/190781a0

59 Cuchillo, C.M., Nogués, M.V. and Raines, R.T. (2011) Bovine pancreatic ribonuclease: fifty years of the first enzymatic reaction mechanism. *Biochemistry* **50**, 7835–7841 doi:10.1021/bi201075b

60 Sorrentino, S., Naddeo, M., Russo, A. and D'Alessio, G. (2003) Degradation of double-stranded RNA by human pancreatic ribonuclease: crucial role of noncatalytic basic amino acid residues. *Biochemistry* **42**, 10182–10190 doi:10.1021/bi030040q

61 Dey, P., Islam, A., Ahmad, F. and Batra, J.K. (2007) Role of unique basic residues of human pancreatic ribonuclease in its catalysis and structural stability. *Biochem. Biophys. Res. Commun.* **360**, 809–814 doi:10.1016/j.bbrc.2007.06.141

62 Lee, J.E. and Raines, R.T. (2003) Contribution of active-site residues to the function of onconase, a ribonuclease with antitumoral activity. *Biochemistry* **42**, 11443–11450 doi:10.1021/bi035147s

63 Pizzo, E., Merlino, A., Turano, M., Russo Krauss, I., Coscia, F., Zanfardino, A. et al. (2011) A new RNase sheds light on the RNase/angiogenin subfamily from zebrafish. *Biochem. J.* **433**, 345–355 doi:10.1042/BJ20100892

64 Nitto, T., Dyer, K.D., Czapiga, M. and Rosenberg, H.F. (2006) Evolution and function of leukocyte RNase A ribonucleases of the avian species, *Gallus gallus*. *J. Biol. Chem.* **281**, 25622–25634 doi:10.1074/jbc.M604313200

65 Pizzo, E., Buonanno, P., Di Maro, A., Ponticelli, S., De Falco, S., Quarto, N. et al. (2006) Ribonucleases and angiogenins from fish. *J. Biol. Chem.* **281**, 27454–27460 doi:10.1074/jbc.M605505200
66 Cho, S. and Zhang, J. (2007) Zebrafish ribonucleases are bactericidal: implications for the origin of the vertebrate RNase A superfamily. *Mol. Biol. Evol.* **24**, 1259–1268 doi:10.1093/molbev/msm047
67 Hooper, L.V., Stappenbeck, T.S., Hong, C.V. and Gordon, J.I. (2003) Angiogenins: a new class of microbicidal proteins involved in innate immunity. *Nat. Immunol.* **4**, 269–273 doi:10.1038/ni888
68 Li, S. and Hu, G.-F. (2012) Emerging role of angiogenin in stress response and cell survival under adverse conditions. *J. Cell. Physiol.* **227**, 2822–2826 doi:10.1002/jcp.23051
69 Lyons, S.M., Fay, M.M., Akiyama, Y., Anderson, P.J. and Ivanov, P. (2017) RNA biology of angiogenin: current state and perspectives. *RNA Biol.* **14**, 171–178 doi:10.1080/15476286.2016.1272746
70 Hoang, T.T. and Raines, R.T. (2017) Molecular basis for the autonomous promotion of cell proliferation by angiogenin. *Nucleic Acids Res.* **45**, 818–831 doi:10.1093/nar/gkw1192
71 Preissner, K.T. (2007) Extracellular RNA. A new player in blood coagulation and vascular permeability. *Hamostaseologie* **27**, 373–377 PMID:18060249
72 Zernecke, A. and Preissner, K.T. (2016) Extracellular ribonucleic acids (RNA) enter the stage in cardiovascular disease. *Circ. Res.* **118**, 469–479 doi:10.1161/CIRCRESAHA.115.307961
73 Lester, S.N. and Li, K. (2014) Toll-like receptors in antiviral innate immunity. *J. Mol. Biol.* **426**, 1246–1264 doi:10.1016/j.jmb.2013.11.024
74 Prüfer, K., Racimo, F., Patterson, N., Jay, F., Sankararaman, S., Sawyer, S. et al. (2014) The complete genome sequence of a Neanderthal from the Altai Mountains. *Nature* **505**, 43–49 doi:10.1038/nature12886
75 Yu, L. and Zhang, Y.-p. (2006) The unusual adaptive expansion of pancreatic ribonuclease gene in carnivora. *Mol. Biol. Evol.* **23**, 2326–2335 doi:10.1093/molbev/msl101
76 Ribó, M., Beintema, J.J., Osset, M., Fernández, E., Bravo, J., De Llorens, R. et al. (1994) Heterogeneity in the glycosylation pattern of human pancreatic ribonuclease. *Biol. Chem. Hoppe Seyler.* **375**, 357–363 PMID:8074810
77 Barrabés, S., Pagès-Pons, L., Radcliffe, C.M., Tabarés, G., Fort, E., Royle, L. et al. (2007) Glycosylation of serum ribonuclease 1 indicates a major endothelial origin and reveals an increase in core fucosylation in pancreatic cancer. *Glycobiology* **17**, 388–400 doi:10.1093/glycob/cwm002
78 Nakata, D. (2015) Increased *N*-glycosylation of Asn^{88} in serum pancreatic ribonuclease 1 is a novel diagnostic marker for pancreatic cancer. *Sci. Rep.* **4**, 6715 doi:10.1038/srep06715